POLITECNICO DI TORINO
Repository ISTITUZIONALE

Parametric thermal-hydraulic analysis of the EU DEMO Water-Cooled Lithium-Lead First Wall using the GETTHEM code

(Article begins on next page)

20 April 2024

Parametric thermal-hydraulic analysis of the EU DEMO Water-Cooled Lithium-Lead First Wall using the GETTHEM code

A. Froio[a]*, A. Del Nevo[b], E. Martelli[b,c], L. Savoldi[a] and R. Zanino[a]

[a]NEMO group, Dipartimento Energia, Politecnico di Torino, 10129 Torino, Italy
[b]ENEA CR Brasimone, 40032 Camugnano, BO, Italy
[c]Università di Roma "La Sapienza", 00185 Roma, Italy
* Corresponding author: antonio.froio@polito.it

Abstract

The system-level code GETTHEM is applied to the thermal-hydraulic analysis of an entire segment of the Water-Cooled Lithium-Lead (WCLL) First Wall (FW) of the EU DEMO reactor, parametrically varying the heat load of the FW and the coolant mass flow rate. The results show that the WCLL FW design can tolerate variations of the distribution of the heat flux with respect to the design value, without requiring modifications. The top inboard and the bottom outboard regions are identified as most critical from the point of view of the cooling of the FW. Finally, the largest possible extent of the WCLL FW surface where the peak heat load can be safely applied is identified through a parametric analysis, performed on the critical regions, to understand which is the limit of the cooling capacity of the system.

1

1. Introduction

One of the challenges of a DEMO reactor is the efficient removal of the heat deposited in the blanket First Wall (FW) by means of a heat transfer fluid, which heats up to produce turbine-grade vapour in a steam generator for the production of electricity. The EU DEMO reactor, see Figure 1, which aims at producing net electrical energy from nuclear fusion by 2050 [1], foresees in its current pre-conceptual design phase different possible solutions for the blanket, which all contain a Breeding Zone (BZ) where a Li-rich material is used to breed tritium. The BZ is inside the Segment Box (SB), which is shown in Figure 2, made in turn by a C-shaped structure alternating the two Side Walls (SWs) with the FW, plus a back-plate. The different blanket solutions under investigation in the EU couple different concepts of BZ to different concepts for the heat removal from the SB. In all cases, the blanket is divided into 18 sectors (according to DEMO 2015 design baseline); each sector contains three Outboard (OB), see Figure 2a-b, and two Inboard (IB) blanket segments resulting in a total of 54 OB and 36 IB segments, respectively.
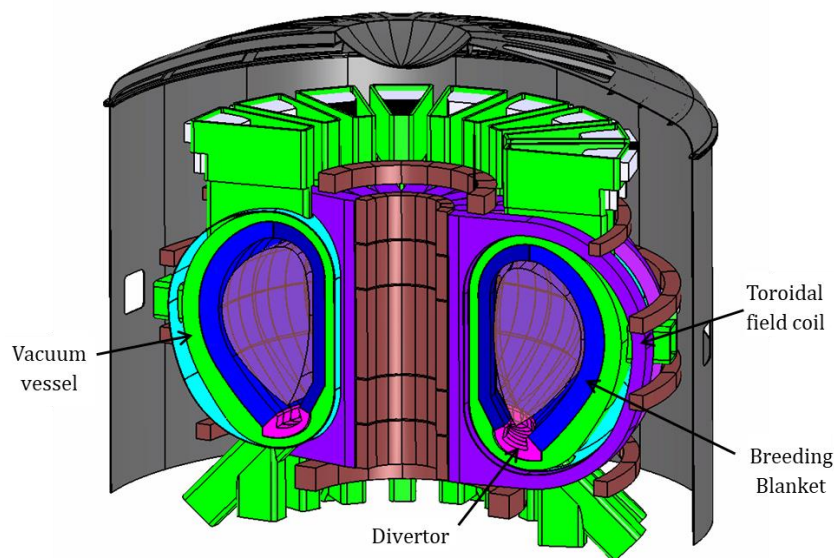

Figure 1: the 2015 baseline of the EU DEMO design; the breeding blanket is the blue-coloured component (reproduced from [2]).

Among the different alternatives, the Water-Cooled Lithium-Lead (WCLL) [3] Breeding Blanket (BB) concept (see Figure 2 and Figure 3) uses water under standard Pressurized Water Reactor conditions (i.e. 155 bar operating pressure and 295-328 °C inlet-outlet temperatures) to cool both BZ and SB, using two fully independent Primary Heat Transfer Systems (PHTS) [4]. The design of the WCLL BB is based on an elementary unit (Figure 3a-b), containing the breeder material, as well as channels and tubes for the proper cooling of BZ and SB, which is repeated in the poloidal direction (see Aection 2 for more details). The nominal mass flow rate distribution among the channels in the different elementary units is determined through an energy balance, starting from the nuclear heat load (which heats both the BZ and the SB) computed by neutronic analyses, plus a uniform heat flux of 290 kW/m² on the FW surface [3], in order to achieve the design outlet temperature in all cooling channels. This 290 kW/m² of FW heat flux is indeed the average design value for all EU DEMO BB concepts until 2016 (i.e. when the most recent WCLL design was developed). Starting from 2017, more detailed specifications have been issued [5]. These provide a non-uniform heat flux distribution detailed in Section 5.

In order to verify the design, a 3D Computational Fluid Dynamic (CFD) analysis was carried out using the available model of the OB equatorial region [3]. Through this analysis it was demonstrated that the zone is capable to fulfil the temperature requirement of the EUROFER ($T_{hotspot} < 550$ °C [6]), used as a structural

material. These results were also used to for the evaluation of the maximum temperature in the structures, as described in Section 4.
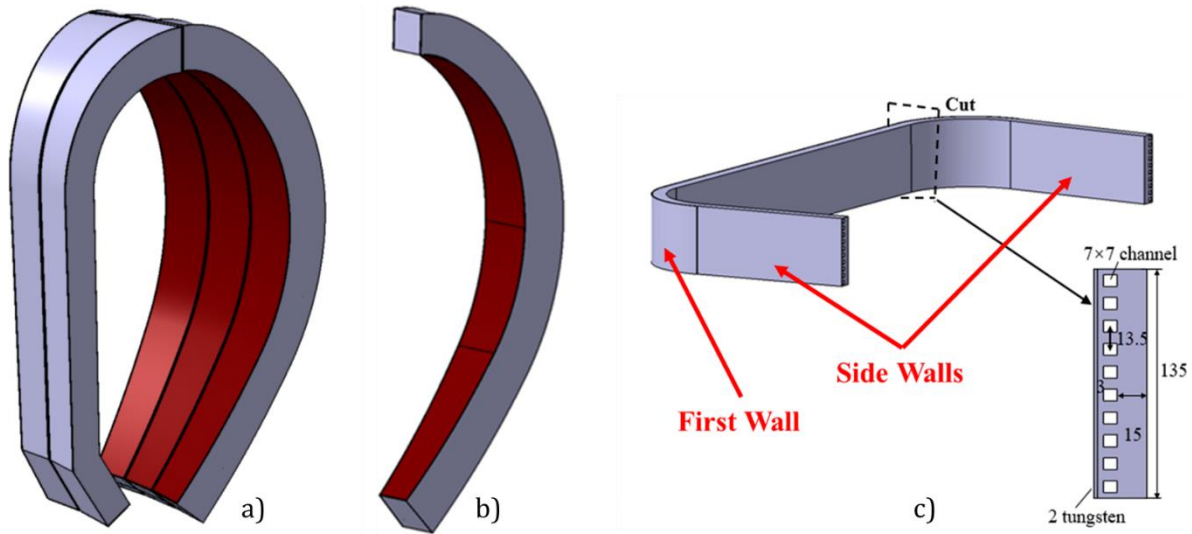

Figure 2: a) a sector of the WCLL breeding blanket; b) a WCLL BB Segment Box, showing the First Wall in red; c) detail of a portion of the SB, showing the Side Walls and the First Wall (adapted from [3]).
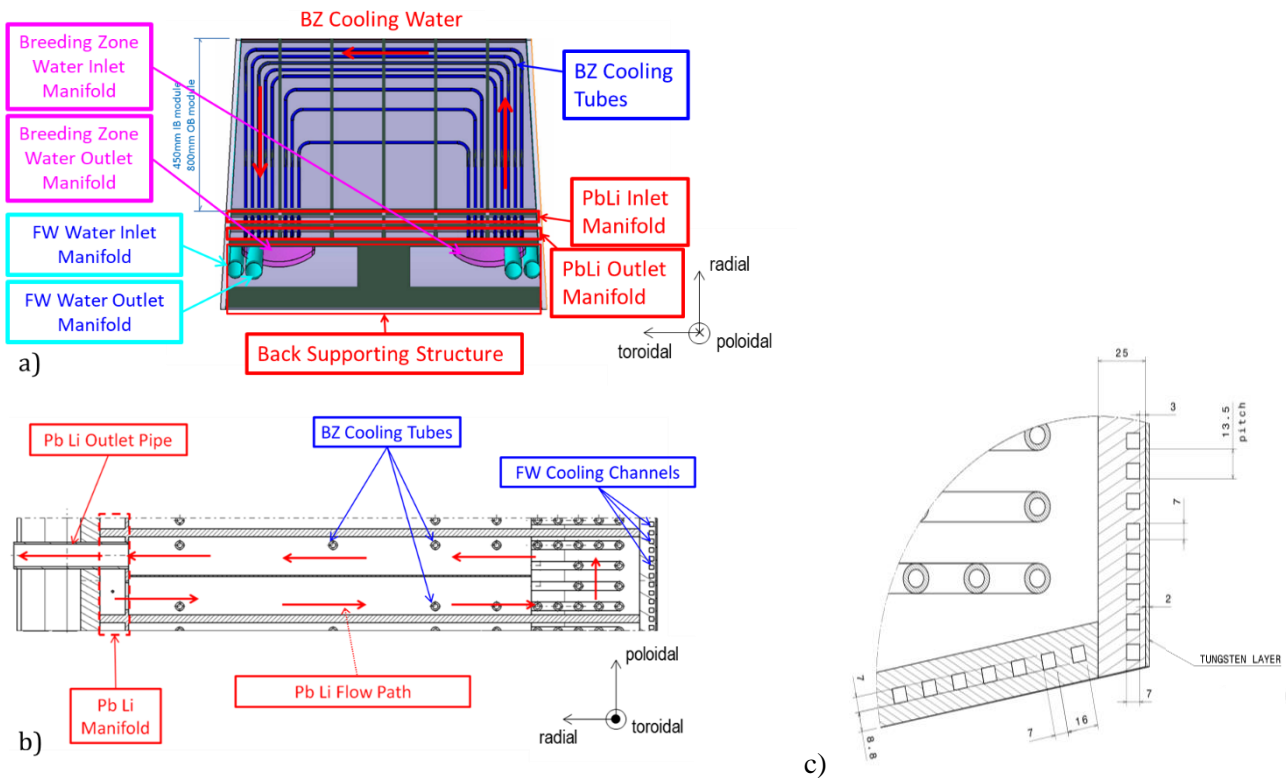
Figure 3: Radial-toroidal (a) and radial-poloidal (b) views of a WCLL elementary unit. (c) Detail of the cross section of the SB, showing the bottom edge of the OB segment, with the square cooling channels (reproduced from [3]).

The GEneral Tokamak THErmal-hydraulic Model (GETTHEM) has been recently developed [7, 8], with the support of the EUROfusion Programme Management Unit, to perform fast system-level thermal-hydraulic transient analyses of the EU DEMO BB PHTS. As a first application, the code was used for the evaluation of T_{hotspot} in the Helium-Cooled Pebble Bed BB [9], while the model for the cooling loops of one elementary unit of the WCLL BB was developed and benchmarked against available CFD simulations [8]. It becomes therefore natural, at this stage, to extend it to the Segment Box of the entire WCLL BB outboard segment.

3

In the present paper, after a brief description of the WCLL current design and of the corresponding GETTHEM model, as well as of the reference map of the heat load on the FW, the GETTHEM model of an entire segment of the WCLL SB is used to evaluate $T_{hotspot}$ in the EUROFER structure and check it against the mentioned 550 °C limit. Parametric thermal-hydraulic analyses, considering the latest FW average heat load specification and different mass flow rate values, are then performed. The analyses have three objectives: 1) to assess the performances of the 2016 WCLL design when the more realistic non-uniform heat flux is applied; 2) to identify the regions where the temperature limits for the structural material are reached; 3) to set-up and qualify (at steady-state level) the thermal-hydraulic model of the SB which will be used for the transient analysis at system level. Finally, the peak heat load specification is applied to increasingly larger portions of the FW, to evaluate the maximum power tolerable by the design in the poloidal coordinate overcoming 550 °C in the EUROFER. Beyond this temperature limit, specific protection measures of the FW, such as those proposed in [10] are needed.

2. The WCLL Breeding Blanket layout

The current design of the WCLL BB is based on the Single Module Segment (SMS) configuration: each blanket segment is a continuous structure, see Figure 2b.

As mentioned, the pre-conceptual design of the WCLL BB is based on a repetitive structure, where the same elementary unit (shown in Figure 3a-b), containing 21 BZ cooling tubes and 10 FW cooling channels (running along the C-shaped structure of the SB), is repeated in the poloidal direction; the elementary units are separated by the toroidal-radial stiffening plates.

The BZ is cooled using double-wall tubes (a sandwich of EUROFER-copper-EUROFER), to reduce the risk of interaction between the PbLi, flowing outside the tubes, and water, flowing inside the tubes. The cross section of a portion of the WCLL SB (related to the bottom edge of the OB segment) is reported in Figure 3c. The FW is made of EUROFER, and the plasma-facing wall is covered with a 2-mm thick tungsten layer. On the internal side, the EUROFER is in direct contact with the PbLi in the BZ. The FW cooling channels are square, see Figure 2c and Figure 3b-c, with a side of 7 mm and a pitch of 13.5 mm; the coolant is distributed to (and collected from) the cooling channels by manifolds in the segment Back Supporting Structure (BSS), see Figure 4, with counter-current flow in adjacent channels. All FW cooling channels in the tokamak are connected to the same loop [4], through the manifolds in the BSS, see Figure 4.
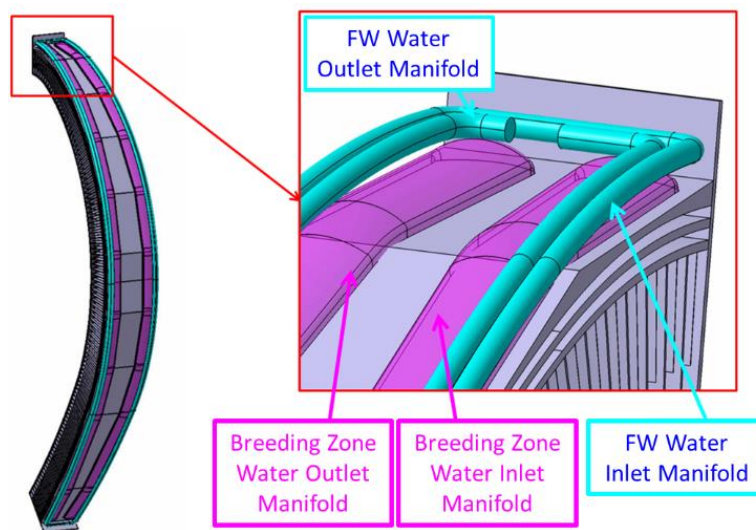

Figure 4: Rear view of a WCLL segment, showing the BSS, with the inlet and outlet manifolds for the SB and BZ coolant (reproduced from [3]).

3.   The GETTHEM WCLL First Wall cooling system model

The GETTHEM model of the WCLL includes two different PHTSs: the SB PHTS and, separately, the BZ PHTS (details on the GETTHEM models can be found in [7, 8, 9]). The activity described in the paper focuses on the SB-PHTS, without considering the ex-vessel components. For the time being, the two PHTSs are designed (and modelled) completely independent, even though – according to the different temperatures – part of the heat deposited onto the SB may be actually removed by the BZ PHTS and vice versa (the fraction of heat that can be transferred between the two is estimated to be upper bound by ~8 %, see [7] and references therein). This assumption is temporarily justified by the aim of keeping GETTHEM fast-running, leading to a rapid identification of the worst conditions through suitable parametric analysis; in addition, this effect of heat transfer is somehow included in the hot-spot temperature estimation procedure developed here, which is described in Section 4 below. It is foreseen, however, to relieve this assumption in future upgrades of the code when needed, trying to reduce as much as possible the increase of the computational cost.

In the GETTHEM model, the SB is discretized in a number of objects equal to the number of FW channels, each including the corresponding volume of EUROFER, as shown in Figure 5. Adjacent channels are thermally coupled through the thermal resistance of the solid in between, see below, while the two solid volumes belonging to neighbouring objects are assumed to be in perfect thermal contact. Each object is discretized in finite volumes (see also Figure 5), which then allow finding an approximate solution of a coupled set of 1D (along the flow direction), transient nonlinear partial differential equations including:

- mass, momentum and energy conservation equations for the fluid. The water coolant is modelled always as a single-phase liquid[1] (no boiling is accounted for), with linearized thermo-physical properties (specific heat, density and internal energy derivative with respect to the temperature) in the entire operational range of the BB (155 bar, 295-328 °C)
- heat conduction for the solid. The thermo-physical properties of the EUROFER are assumed constant and equal to the average values in the temperature range of interest (295-550 °C).

The heat transfer coefficient (HTC) between solid (wall) and liquid is also taken as a constant, i.e., the average HTC computed with the Dittus-Bölter correlation in the operational range; the volume-averaged solid temperature is then computed from the wall temperature, through a conductive resistance, assuming constant conductivity as stated above (see [7, 9] for details). The local variation of the HTC, due e.g. to fluid acceleration or subcooled nucleate boiling, is neglected in the model: the reason behind this choice is again to keep the code fast-running, considering also that such effects are always increasing the HTC (hence neglecting them is conservative)[1]. It has been estimated (through simulations comparing GETTHEM results with more detailed models) that all these assumptions produce an error below 3 % in terms of temperature increase for steady-state analyses, as in this case [11]; the effect of these assumptions in transient conditions is not estimated yet.

---

[1] This assumption is consistent because local subcooled nucleate boiling conditions are expected, on the opposite departure from nucleate boiling (and the consequent heat transfer degradation) is excluded if the maximum temperature limit of the EUROFER is fulfilled.
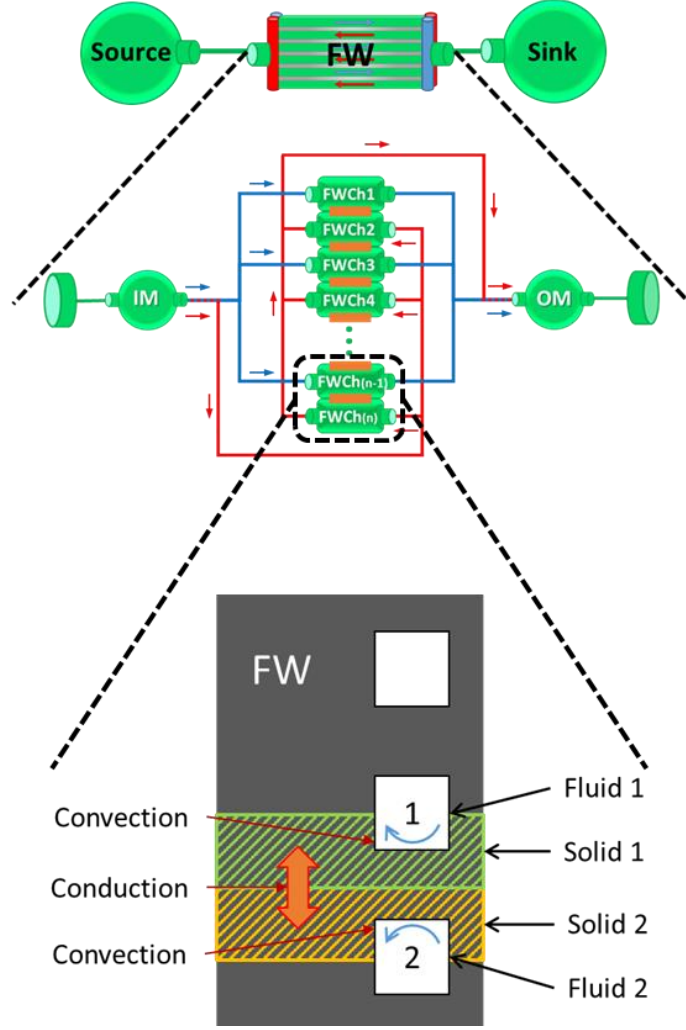
Figure 5: Sketch of the GETTHEM WCLL SB PHTS model, showing the detail of the FW component and the heat transfer mechanisms accounted for in the solid finite volumes (IM/OM: Inlet/Outlet Manifold).

4. Evaluation of $T_{hotspot}$

As a system-level model, GETTHEM can directly compute only average temperatures in the finite volumes; so, a procedure has been developed to estimate the hot-spot temperature in the EUROFER in the postprocessing phase. An accurate estimate of $T_{hotspot}$ can be obtained through the evaluation of a "peaking factor" f_p^{CFD}, which can be obtained in turn by 3D CFD studies on the elementary unit, see Figure 6. The adopted procedure, already successfully benchmarked and applied to the HCPB [9], is sketched in the flowchart reported in Figure 7.

Starting from the left part of the flowchart in Figure 7, the value of f_p^{CFD} is computed from the post-processing of the CFD results on an elementary cell, which includes 10 channels, according to

$$f_p^{CFD} = \frac{T_{hotspot}^{CFD} - T_{H_2O,in}}{T_{ave}^{CFD} - T_{H_2O,in}} \tag{1}$$

where $T_{hotspot}^{CFD}$ is the computed hotspot temperature in the EUROFER computational domain, T_{ave}^{CFD} is the volume-averaged temperature in the EUROFER domain (limited to the FW and excluding the side walls, see dashed region in Figure 6) and $T_{H_2O,in}$ is the water inlet temperature (295 °C), taken as a reference temperature. In order to take into account the steeper temperature gradient deriving from a larger heat flux, different CFD simulations have been performed, keeping all the parameters constant (i.e. geometry and coolant mass flow

rate) except the heat flux on the FW, which has been varied in the range 200÷1200 kW/m². From these results, a linear correlation for f_p^{CFD} has been obtained as

$$f_p^{CFD}(q'') = 1.58 \times q'' + 0.960 \tag{2}$$

with q'' in MW/m², which best fits the CFD-computed values, see Figure 8. The value of the peaking factor has also a weak dependence on the mass flow rate: this was evaluated for the OB central segment zone geometry lower than 5 %, varying the mass flow rate in the range 10 g/s – 25 g/s per channel, and keeping the heat flux constant; consequently, this weak dependence has been neglected hereafter.
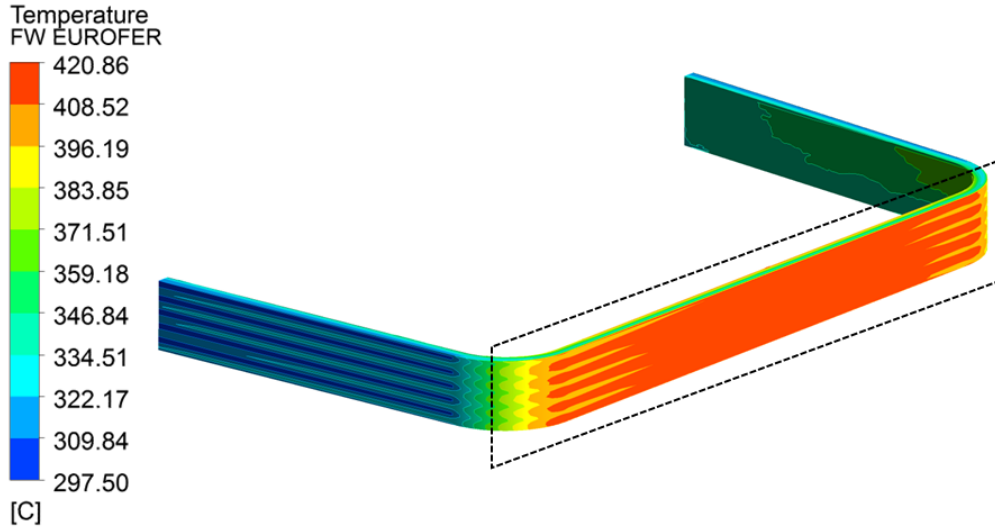
Figure 6: Temperature map on the SB surface, according to the 3D CFD study. The dashed rectangle indicates the region used to determine the peaking factor (i.e. the FW).

Figure 7: Flow chart for the estimation of the EUROFER hotspot temperature.

As sketched in the right part in Figure 7, the hotspot temperature $T_{hotspot}^{GETTHEM}$ can then be estimated postprocessing the GETTHEM results according to

$$T_{hotspot}^{GETTHEM} = T_{H_2O,in} + f_p^{CFD}\left(T_{ave}^{GETTHEM} - T_{H_2O,in}\right) \tag{3}$$

7

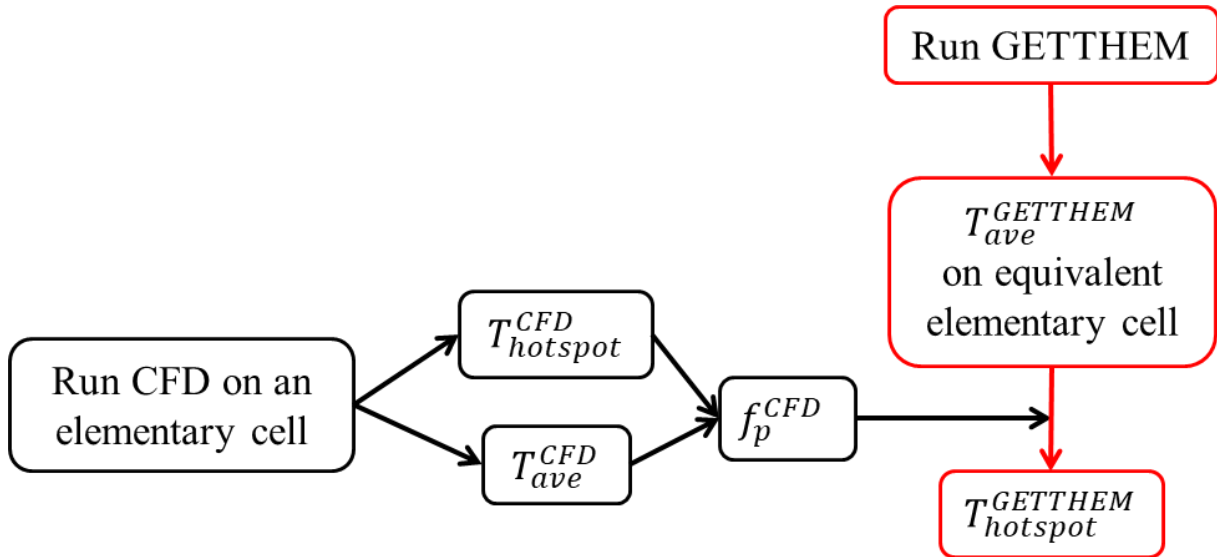where $T_{ave}^{GETTHEM}$ is the temperature computed in the FW solid finite volumes by GETTHEM, averaged in 10 adjacent channels to be consistent with the CFD studies on which f_p^{CFD} is based on. It should be noted that the heat transfer between the SB and BZ is taken into account in the CFD analyses. Therefore, the evaluated peaking factor accounts also for this process, which is neglected in the GETTHEM model.
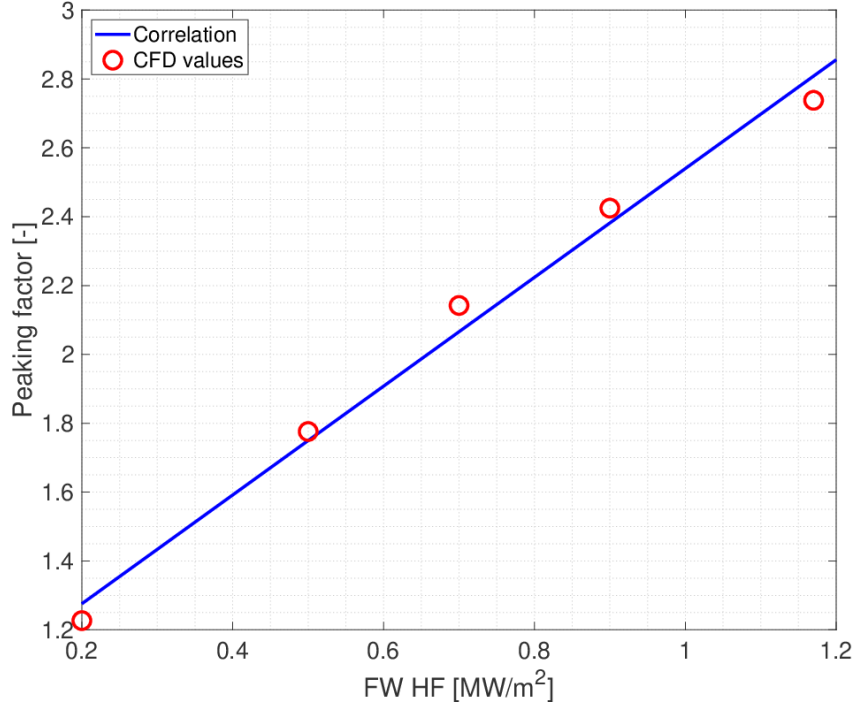

Figure 8: Correlation of the peaking factor with the FW heat flux and comparison with the values extracted from CFD.

5. Scenarios

The scenarios analysed deal with different combinations of mass flow rates and coolant HTC, as explained below. The simulations are driven by the nuclear power deposition, acting on both SB and BZ, and the heat load coming from the plasma, acting on the FW. The nuclear volumetric power density is assumed as specified in [12].

For the plasma heat load, the most recent poloidal distribution provided by the EUROfusion Programme Management Unit (PMU) [5] is used[2]. This heat flux distribution is, however, determined based on a FW configuration (reported in Figure 9a), which is somewhat different from the WCLL one, i.e. having a different poloidal shape, a multi-module segment approach and also a central OB segment different from the other two, being based on the 2017 EU DEMO design. To overcome this issue, the heat load of the FW is rescaled distributing the different heat loads on the portions of the WCLL single-module segment FW corresponding to the different modules, as shown in Figure 9b. Since the OB segments in the WCLL design are all identical, the total power on the three "PMU" segments has been simply divided by 3, to obtain a heat flux related to the "average" segment. These are of course rough assumptions, as the heat load coming from the plasma is strongly anisotropic and depends heavily on the FW shape itself. Indeed, as clearly stated in [5], the FW heat load specification computed by the PMU can be considered valid only for the 2017 EU DEMO FW shape. Nevertheless, the aim of this work is *not* to determine what would be the correct heat load distribution, but to analyse the robustness of the design of the WCLL cooling system, i.e. to identify how much a deviation in the heat load from the design specification would affect the cooling performance; consequently, this "roughly reshaped" heat load distribution is used in the present work. The resulting heat flux distribution is reported in

---

[2] Note that this is not the input used for the design of the WCLL, which is instead a uniform heat flux of 290 kW/m², as mentioned above.

Figure 10. In [5], in addition to the average heat flux, also the peak value is reported, which can be deposited on small portions of the FW (without affecting the total power deposition); these peak values are shown in Figure 10 as well.

a) b)

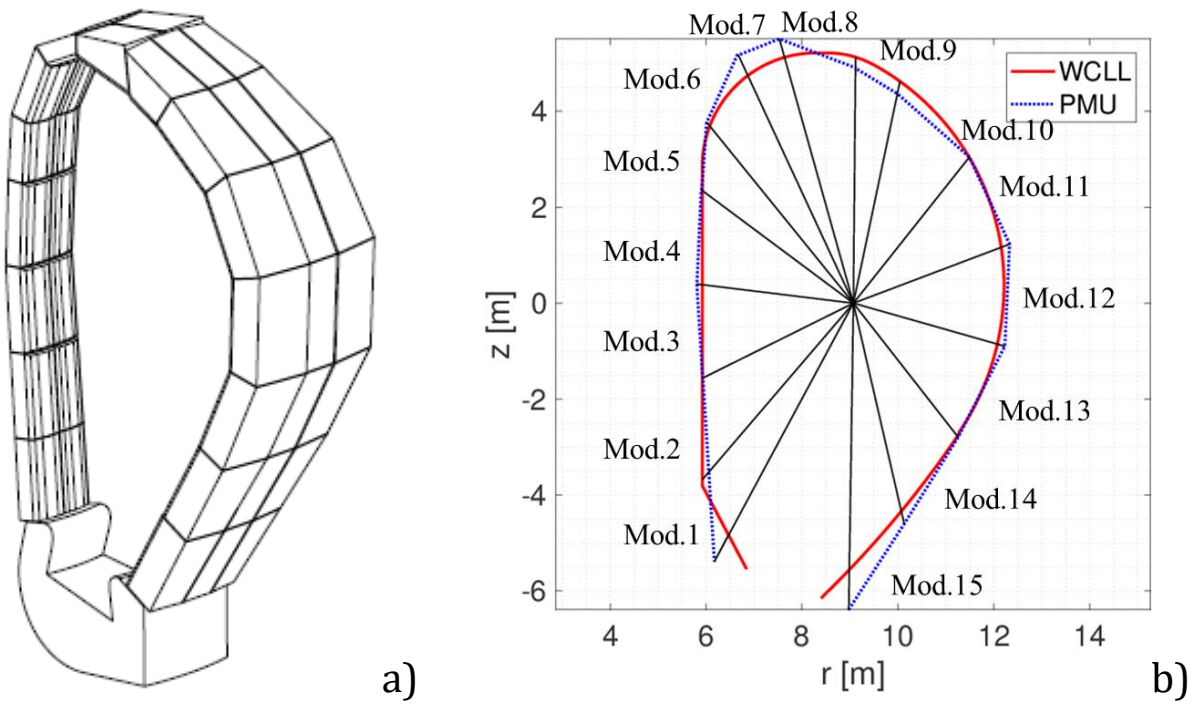Figure 9: (a) 3D FW geometry used by the EUROfusion PMU to compute the plasma heat flux [13]. (b) Comparison of the poloidal profiles of the WCLL (solid line) and PMU (dashed line) FWs; the poloidal profile of the PMU FW refers to the middle of the central OB segment, whereas the WCLL one is the same for all toroidal locations.
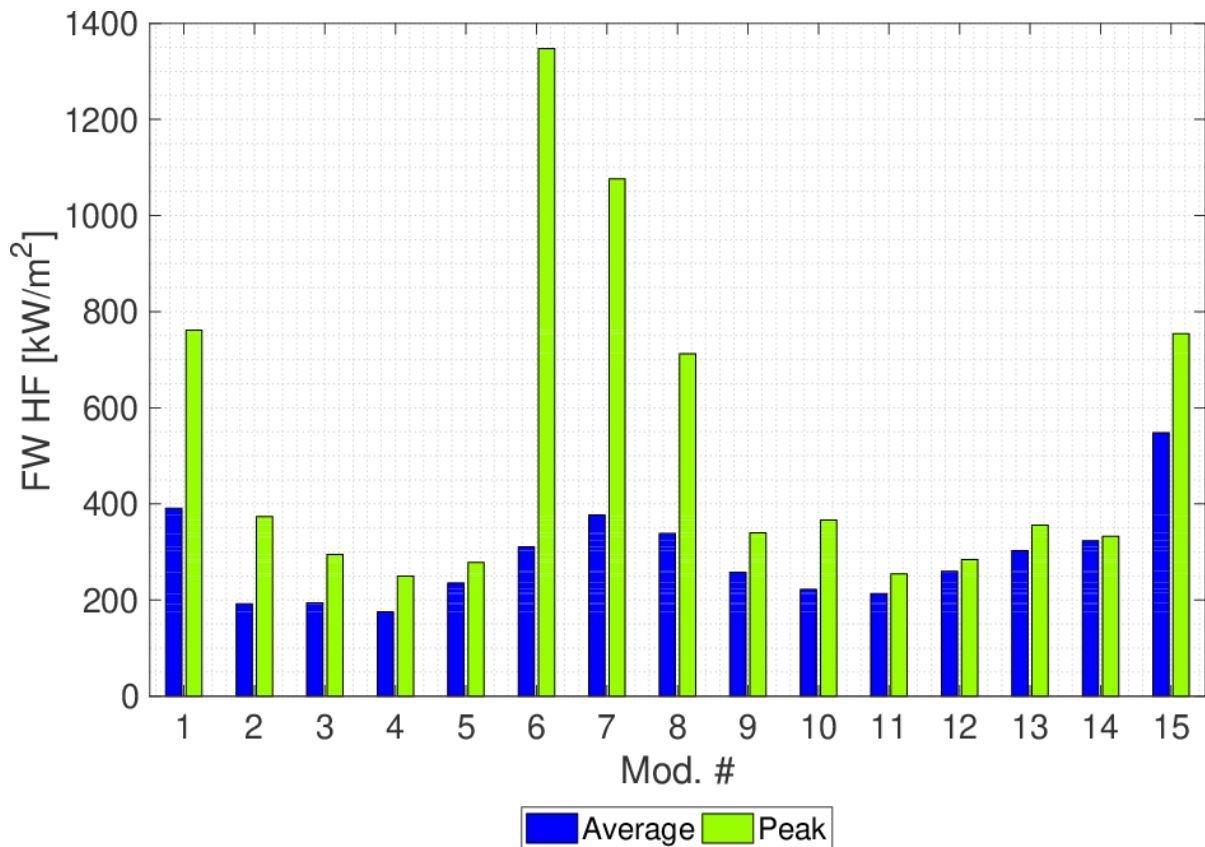

Figure 10: Average and peak plasma heat flux to the FW surface.

9

Looking at Figure 10, it is evident that the heat flux distribution among the modules is non-uniform, with the largest loads on the top and bottom parts of the FW (Mods. 1, 6-8 and 15). When applying the PMU average heat flux, the total power to the entire segment increases with respect to the WCLL design value by ~25 % on the IB (going from 3.26 MW to 4.08 MW) and by ~19 % on the OB (from 6.49 MW to 7.71 MW).

As far as the coolant mass flow rate is concerned, different alternatives are considered:

- the WCLL design distribution (red dashed line in Figure 11b);
- a mass flow rate distributed according to the power distribution resulting from the PMU average heat flux (blue line in Figure 11), keeping the total mass flow rate equal to the WCLL design value;
- a mass flow rate distribution computed in order to have a uniform outlet temperature, equal to the design value of 328 °C, according to equation (4) below.

As far as the HTC is concerned, as already mentioned, the average HTC is computed in the temperature range (295-328 °C); then, the minimum value among all the channels (according to the different mass flow rates) is used for the entire segment. This conservative assumption, made for the sake of simplicity, has a negligible effect on the results: to prove this statement, in one of the simulated scenarios the average value will be used, as explained below.

The scenarios considered are summarized in Table 1; the distribution of the relevant parameters (heat load, HTC and mass flow rate) in Scenarios 1-4 is also reported in Figure 11.

All scenarios considered here are modelled as steady-state, as these loads are constant during the plasma burn phase, which lasts much longer than the characteristic times of the cooling system, see [7, 9] and references therein.

Table 1: List of the analyzed scenarios. In all scenarios, the heat load is distributed according to the PMU average HF.

Scenario	Mass flow rate	HTC
1	Total value and distribution according to design data	**Average** value
2	Total value and distribution according to design data	**Minimum** value
3	Total value according to design data, distribution according to PMU power specifications	
4	Total value and distribution recalculated according to PMU power specifications	

As mentioned above, the aim of Scenarios 1 and 2 is to check the effect of different HTCs: the average value among all the channels in the segment is used in Scenario 1, whereas the minimum value is used in Scenario 2 (conservative assumption).

In Scenario 3, the same total mass flow rate is used (16.8 kg/s IB, 33.5 kg/s OB), but it is redistributed to the channels according to the PMU average power distribution, in order to have a uniform outlet temperature. In Scenario 4, also the total mass flow rate is changed according to equation (4)

$$\dot{m}_i = \frac{\dot{Q}_i}{h_{out} - h_{in}} \tag{4}$$

where $\dot{m}_i$ is the mass flow rate in the i-th channel, $\dot{Q}_i$ is the power deposited in the i-th channel, h_{out} is the outlet enthalpy at 328 °C and h_{in} is the inlet enthalpy at 295 °C, so that the outlet temperature distribution is

uniformly equal to the design value (328 °C). The aim is to have here a base case, which keeps the structures at a temperature below the limit, while at the same time allowing the Balance-of-Plant to work in its design conditions.

Finally, keeping the mass flow rate distribution as in Scenario 4, a parametric analysis is performed, applying the peak heat flux only to an increasing number of channels in each region (uniformly on the channel length), until the $T_{hotspot}$ overcomes 550 °C.
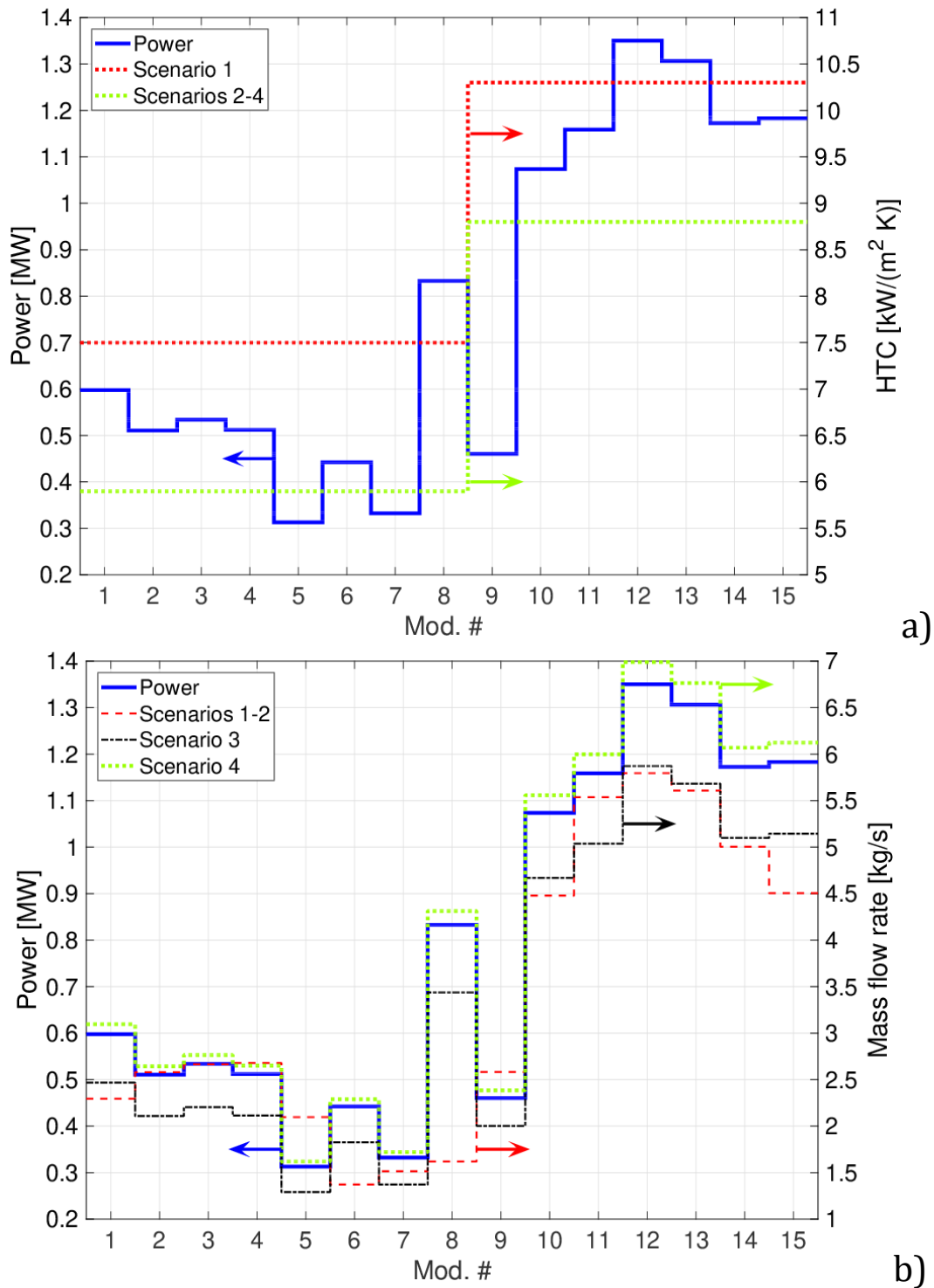

Figure 11: Poloidal distribution of the total heat load on each module (solid lines, left axes), HTC (dashed lines, right axis in a) and mass flow rate (dashed lines, right axis in b), for all the scenarios analysed in this work.

11

6.   Results

6.1.   Scenarios 1-4

The analyses are conducted assessing the results on the basis of the following design constraints: the $T_{hotspot}$ in the structures, which shall stay below 550 °C as mentioned; and the water bulk temperature, which by design shall never overcome the saturation temperature and shall ensure the margin from departure from nucleate boiling. Figure 12 reports the distribution of the $T_{hotspot}$ in a WCLL Segment Box, for the four scenarios. As expected, the most critical point is in the region of Mod. 8, where the heat flux (and total power, consequently) causes an overheating of the structures; nevertheless, the $T_{hotspot}$ never overcomes the limit, not even when using the design mass flow rate distribution, with always more than 100 °C of margin. For Scenarios 1-2, the model computes in Mod. 6 and Mod. 8 a temperature larger than the water saturation temperature at the given pressure, so that its predictions are inaccurate, albeit conservative[3]. This is a consequence of the use of the nominal mass flow rate to try removing a power larger (by ~20 %) than the nominal value, leading to a larger temperature increase in the coolant, eventually causing saturation and in the extreme case critical heat flux. It should be remarked, however, that Scenarios 1-2 are far from nominal operating conditions; nevertheless, GETTHEM has been used to point out that in this condition the design criterion concerning the water saturation temperature is not met, and to identify where more detailed analyses are needed.

In Scenarios 3-4, instead, both IB and OB segments are below the temperature limit in all the points, with Mod. 6 and Mod. 8 still containing the hotspots, and also independent of two-phase flow, as the computed temperature never reaches saturation.

More in detail, the comparison of Scenarios 1-2 shows that the conservative assumption on the HTC causes a modest increase of $T_{hotspot}$ (~7 %); moreover, both IB and OB segments have in all scenarios a large margin with respect to the temperature limit, always above 100 °C. Also, on the OB the $T_{hotspot}$ distribution is almost uniform at ~355°C, with only Mod. 15 reaching higher temperatures due to the larger heat flux.

In all the scenarios, a macroscopic difference in the behaviour is found between OB and IB. In particular, the $T_{hotspot}$ distribution in the IB is piecewise constant, following the piecewise constant heat load distribution, with the exception of a few channels at the interface between the different "modules". Conversely, on the OB the temperature distribution is more uniform and it has a concave shape. The reason for this behaviour is found in how the different channels are coupled in the model: as mentioned in Section 3 above (and better explained in [7, 9]), this is done through thermal resistances, whose values are determined according to the geometry and to the EUROFER thermal conductivity. Because of the different dimensions of OB and IB, the resistance between the OB channels is smaller than that between the IB channels, causing the temperature distribution to homogenize and nearby "modules" to affect each other. Indeed, the concavity is found also in the IB temperature distribution (i.e. it is not exactly piecewise constant), but it is less visible, in view of the smaller thermal coupling between neighbouring channels.

If the mass flow rate is adapted according to equation (4) in order to match the new total power (and the related distribution), as in Scenario 4, the entire BB is below the operational limit by at least ~180 °C everywhere; this is also compliant with the Balance-of-Plant design, as the outlet temperature is now everywhere equal to the design value of 328 °C (Figure 13). For this reason, this scenario is assumed as a reference case for the parametric analysis, which will be presented in the next section.

---

[3] Such predictions are in fact not assuming constant fluid temperature in the bulk while boiling, nor considering the increase of HTC associated with the onset of nucleate boiling.
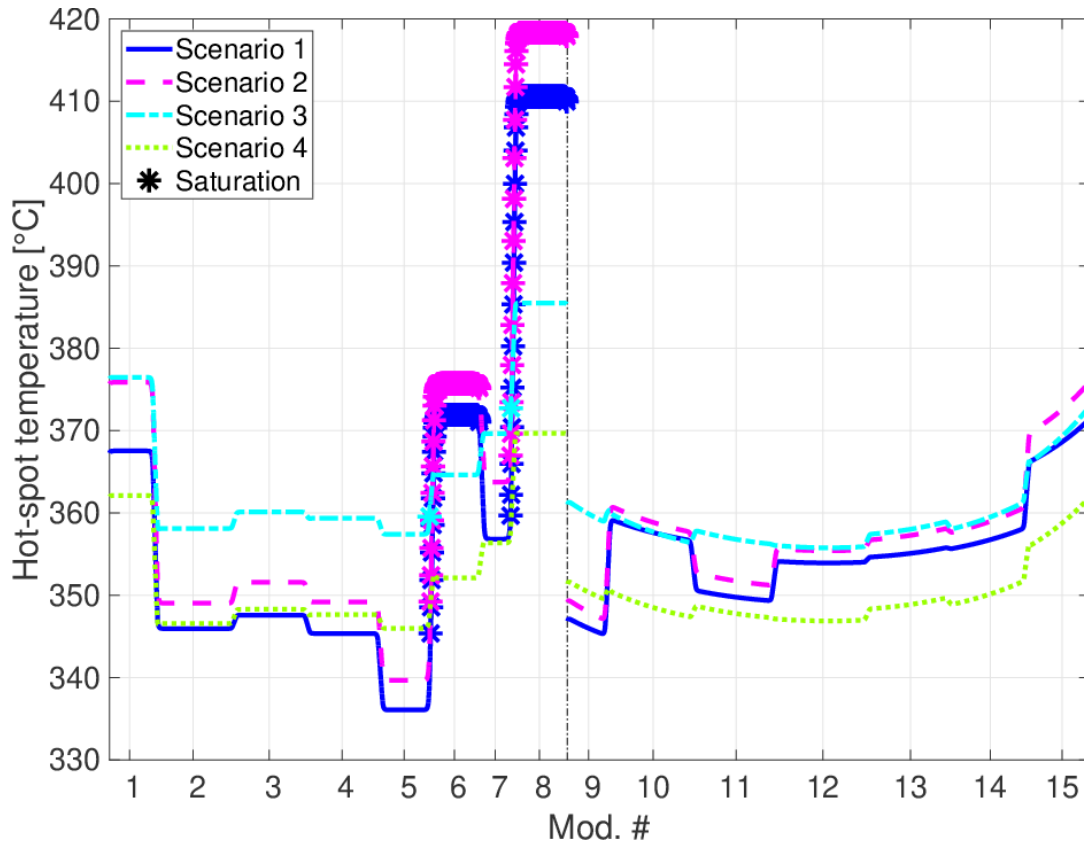
Figure 12: Poloidal distribution of the hotspot temperature for Scenarios 1-4. Points marked with a star correspond to locations where saturation was detected by the model.
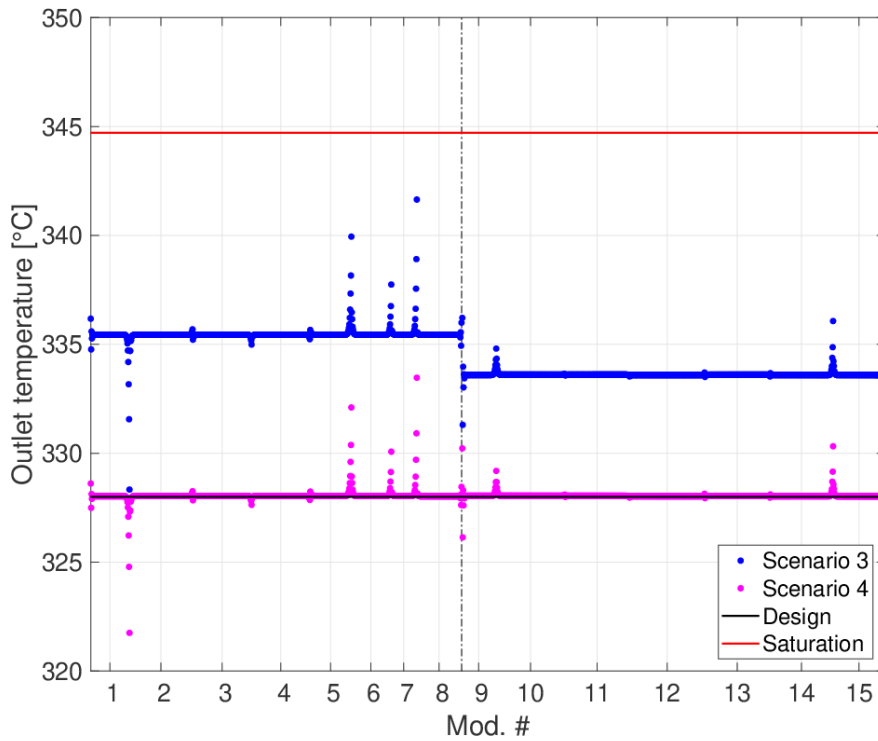

Figure 13: Poloidal distribution of the outlet temperature from the WCLL FW cooling channels, for Scenarios 3 and 4. The thin red line represents the saturation temperature, whereas the thin black line represents the design outlet temperature (328 °C).

6.2. Parametric analysis

Starting from Scenario 4, the peak heat flux (keeping the nuclear heat load constant) is applied on the WCLL FW, in order to identify the largest possible surface, which can be loaded with this value without causing overheating above 550 °C. Since the total power generated in the plasma is kept constant, when applying this peak heat flux to some channels, the heat load to the other channels is reduced. This parametric analysis is performed only on the critical regions, which are identified *a priori* applying the peak heat flux over the entire region (which is an over-conservative scenario). As a consequence, only Mods. 1-2, 6-8, 10 and 15 are analysed, as in all the other regions the $T_{hotspot}$ does not overcome 550 °C even in this over-conservative scenario and no saturation is detected.

The peak heat flux is then applied to an increasing number of channels (uniformly distributed along the plasma-facing channel length) in the regions of Mod. 1-2, 6-8, 10 and 15, to understand what should be the maximum extent of the region which could be "safely" subject to the peak flux (i.e., keeping the EUROFER temperature below the limit or the maximum fluid temperature below saturation). The peak heat flux is imposed in channels in the middle of the region, with the exception of Mod. 15 where the last channels (i.e. the bottom ones) are loaded with the peak value, as they are expected to be more critical (see Figure 12 above).

The results of this analysis are reported in Table 2: the most critical region is found to be Mod. 6, which is not surprising as the peak heat flux in that region is ~1.4 MW/m². In this region, in fact, both coolant saturation occurrence and EUROFER temperature exceeding the limit are calculated if a single channel is loaded with the peak heat flux. The result is not much different in Mod. 8, where the EUROFER temperature overcomes 550 °C also when loading a single channel, and saturation conditions are detected when two channels are loaded. The situation is not better in the other IB regions under investigation, as it is sufficient to load four channels with the peak heat flux to reach at least one of the two conditions (in Mod. 2 the hot-spot temperature never overcomes 550 °C, even if all the channels are loaded with the peak heat flux).

Coming to the OB, as expected from the previous results a better performance is calculated: in Mod. 10, saturation conditions are found when loading at least 8 channels with the peak heat flux, whereas the $T_{hotspot}$ never reaches 550 °C even when loading all the channels with the peak heat flux. In Mod. 15, instead, saturation conditions are never found, and the EUROFER limit is overcome in the last channel (by 0.7 °C), when the last 9 channels are loaded with the peak heat flux. However, the constraint is violated only in a small portion of the OB segment, and the hot-spot temperature reached is only marginally above the limit.

The results evidence the need to have a protection system to mitigate the temperature of the EUROFER in poloidal positions corresponding to Mod. 6 and 8. Conclusions on the other zones require the detailed heat flux morphology on the structures.

As a final remark, it should be stressed that the results reported in Table 2 are conservative if considering the assumptions about the heat transfer between the coolant and the solid. This would become even more important at high heat fluxes, where onset of nucleate boiling conditions will take place, causing an increase of the heat transfer. The effect of the coupling between the Segment Box and the Breeding Zone is instead trickier to analyse, as the heat transfer may take place in both directions according to the different temperature (e.g. it may be different at different poloidal locations). To properly assess this effect, a GETTHEM analysis of the coupled circuits is envisaged in the future. In addition, considering the model simplifications, a detailed (e.g. 3D CFD) analysis could be carried out, exploiting these results to focus only on the conditions identified as limiting in Table 2.

Table 2: Results of the parametric analysis.

Region	Number of channels loaded with peak heat flux which cause:	
	Saturation	$T_{hotspot} > 550\ °C$
Mod. 1	3	6
Mod. 2	5	-
Mod. 6	1	1
Mod. 7	2	4
Mod. 8	2	1
Mod. 10	8	-
Mod. 15	-	9

7.   Conclusions and perspective

The GETTHEM system-level thermal-hydraulic code has been applied to analyse the hot-spot temperature distribution in the WCLL BB Segment Box. The most recent First Wall heat flux distribution, as computed by the EUROfusion PMU, has been rescaled and adapted to the 2016 WCLL design and DEMO 2015 baseline, and applied to the WCLL FW, considering different distributions of the mass flow rate.

The analyses have three objectives: 1) to assess the performances of the 2016 WCLL design when the more realistic non-uniform heat flux is applied; 2) to identify the regions where the temperature limits for the structural material are reached; 3) to set-up and qualify (at steady-state level) the thermal-hydraulic model of the SB which will be used for the transient analysis at system level.

The analysis showed that the WCLL design is flexible enough to guarantee adequate cooling of the SB, and that it would be possible with a small increase of the mass flow rate to keep the coolant outlet temperature at the design value. On the other hand, a parametric analysis with the peak heat flux showed that most of the BB is within the design constraints even if loaded with a much larger total power, with the exception of the most critical IB regions far from the equatorial plane.

In perspective, the results of the analysis motivate the need for more detailed studies in the most critical regions (e.g. CFD or critical heat flux investigations). Exploiting the result of such simulations, the GETTHEM approach to the computation of the hot-spot temperature, which depends on available 3D temperature distributions evaluated either by codes or experimental data, is improved. On the other hand, it is foreseen to improve the GETTHEM modelling of some phenomena, such as the subcooled nucleate boiling and the thermal coupling between the SB and BZ cooling circuits, to increase the range of applicability of the model.

Acknowledgements

References

[1] F. Romanelli, P. Barabaschi, D. Borba, G. Federici, L. Horton, R. Neu, D. Stork and H. Zohm, "Fusion Electricity – A roadmap to the realisation of fusion energy," European Fusion Development Agreement (EFDA), 2012, ISBN 978-3-00-040720-8T. [Online]. Available: https://www.euro-fusion.org/wpcms/wp-content/uploads/2013/01/JG12.356-web.pdf.

[2] R. Wenninger and G. Federici, "DEMO1 Reference Design - 2015 April ("EU DEMO1 2015")," EFDA_D_2LBJRY, 2015.

[3] E. Martelli, A. Del Nevo, P. Arena, G. Bongiovì, G. Caruso, P. A. Di Maio, M. Eboli, G. Mariano, R. Marinari, F. Moro, R. Mozzillo, F. Giannetti, G. Di Gironimo, A. Tarallo, A. Tassone and R. Villari, "Advancements in DEMO WCLL breeding blanket design and integration," *International Journal of Energy Research,* vol. 42, no. 1, pp. 27-52, 2017.

[4] E. Martelli, F. Giannetti, G. Caruso, A. Tarallo, M. Polidori, L. Barucca and A. Del Nevo, "Study of EU DEMO WCLL Breeding Blanket and Primary Heat Transfer System Integration," *Fusion Engineering and Design,* 2018 (in press).

[5] F. Maviglia, "DEMO PFC Heat Load Specifications," EFDA_D_2NFPNU v0.3, 2017.

[6] L. V. Boccaccini, L. Giancarli, G. Janeschitz, S. Hermsmeyer, Y. Poitevin, A. Cardella and E. Diegele, "Materials and design of the European DEMO blankets," *Journal of Nuclear Materials,* Vols. 329-333, part A, pp. 148-155, 2004.

[7] A. Froio, C. Bachmann, F. Cismondi, L. Savoldi and R. Zanino, "Dynamic thermal-hydraulic modelling of the EU DEMO HCPB breeding blanket cooling loops," *Progress in Nuclear Energy,* vol. 93, pp. 116-132, 2016.

[8] A. Froio, F. Casella, F. Cismondi, A. Del Nevo, L. Savoldi and R. Zanino, "Dynamic thermal-hydraulic modelling of the EU DEMO WCLL breeding blanket cooling loops," *Fusion Engineering and Design,* vol. 124, pp. 887-891, 2017.

[9] A. Froio, F. Cismondi, L. Savoldi and R. Zanino, "Thermal-hydraulic analysis of the EU DEMO Helium-Cooled Pebble Bed Breeding Blanket using the GETTHEM code," *IEEE Transactions on Plasma Science,* vol. 46, no. 5, pp. 1436-1445, 2018.

[10] F. Cismondi, L. V. Boccaccini, G. Aiello, J. Aubert, T. Barrett, C. Bachmann, L. Barucca, E. Bubelis, S. Ciattaglia, A. Del Nevo, E. Diegele, M. Gasparotto, G. Di Gironimo, P. A. Di Maio, F. A. Hernández, G. Federici, I. Fernández-Berceruelo, T. Franke, A. Froio, C. Gliss, J. Keep, A. Loving, E. Martelli, F. Maviglia, I. Moscato, R. Mozzillo, Y. Poitevin, D. Rapisarda, L. Savoldi, A. Tarallo, M. Utili, L. Vala, G. Veres and R. Zanino, "Progress in EU Breeding Blanket design and integration," *Fusion Engineering and Design,* 2018 (in press).

[11] A. Froio, "Multi-scale thermal-hydraulic modelling for the Primary Heat Transfer System of a tokamak," PhD Thesis, 2018. [Online]. Available: http://hdl.handle.net/11583/2704378.

[12] A. Del Nevo, E. Martelli, P. Agostini, P. Arena, G. Bongiovì, G. Caruso, G. Di Gironimo, P. A. Di Maio, M. Eboli, R. Giammusso, F. Giannetti, A. Giovinazzi, G. Mariano, F. Moro, R. Mozzillo, A. Tassone, D. Rozzia, A. Tarallo, M. Tarantino, M. Utili and R. Villari, "WCLL breeding blanket design and integration for DEMO 2015: status and perspectives," *Fusion Engineering and Design,* vol. 124, pp. 682-686, 2017.

[13] M. Kovari, F. Maviglia and T. R. Barrett, "DEMO 2016 - First Wall," EFDA_D_2MWN32 v1.0, 2016.